

# Hebbian plasticity assisted robust desynchronization in simplicial complexes

Ajay Deep Kachhvah\* and Sarika Jalan†

Complex Systems Lab, Department of Physics, Indian Institute of Technology Indore - Simrol, Indore - 453552, India

The plasticity in higher-order coupling interaction, best encoded by an adaptive simplicial complex structure, may significantly affect the synchronization dynamics. Here, we investigate the impact of adaptation in the 2-simplex (triadic) coupling on the nature of the transition to desynchrony in the networked oscillators. The adaptation in triadic coupling takes a cue from the Hebbian learning rule, i.e., the coupling weight of a triad is prone to increase if the oscillators forming the triad are in phase and decrease if they are out of phase. The triadic coupling weights adapting through the Hebbian learning mechanism give rise to a first-order route to desynchronization as observed in the case of static triadic coupling; however, its onset is entirely regulated by the Hebbian learning parameters. The fact that the Hebbian learning parameters govern the onset of desynchronization is supported by rigorous mean-field analysis.

## I. INTRODUCTION

For decades, consideration of the pairwise interaction between different networked dynamical units has been at the forefront to capture the underlying dynamics affecting distinct dynamical processes on various physical and biological complex systems. However, complex systems such as brains [1, 2] and social interaction networks [3, 4] have the underlying topology of higher-order connections, which can be framed using simplicial complexes [5, 6]. A simplicial structure may include simplices of different dimensions, namely, vertices (0-simplex), edges (1-simplex), triangles (2-simplex), tetrahedrons (3-simplex), etcetera to apprehend the higher-order interactions among the units of a complex system. Recently modeling many-body interactions using simplicial complexes, either alone or along with pairwise interaction, is gaining momentum to feature the role of these interactions on various dynamical processes [7–17].

The adaptation is at the backbone of the construction and functioning of many physical and biological complex systems. Experimental findings in neuroscience have lead to an impression that the synaptic plasticity between the interacting neurons is at the rationale of the learning process and long-term memory in the human brain [18, 19]. Hebb [20] first conceptualized the fact that the synaptic strength between two interacting neurons is strengthened (weakened) if they are simultaneously firing (not firing), which was later supported by experimental evidence [19, 21, 22]. Further, a neural network can be represented by an ensemble of phase oscillators by encoding the relative spike timing of presynaptic and postsynaptic spikes of the interacting neurons in terms of phases. Thus, the plasticity of the neural network materializes through the adaptation of the synaptic strength between two interacting neurons. The systems of phase oscillators incorporating plasticity in the connection strength

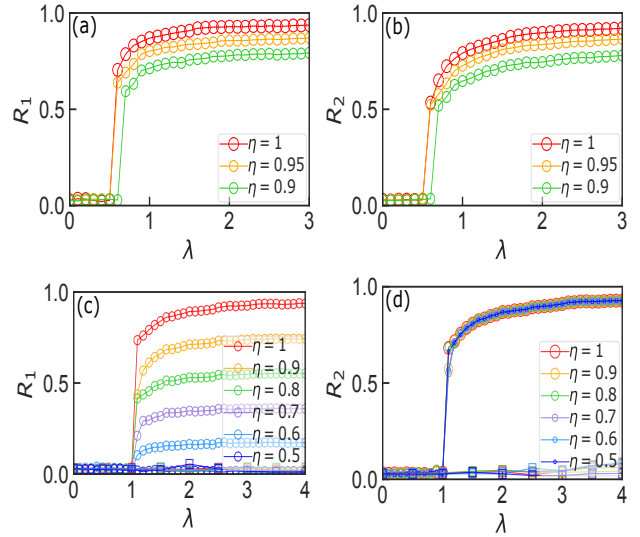


FIG. 1. (Color online) Robustness of critical coupling against phase asymmetry  $\eta$ :  $R_1-\lambda$  and  $R_2-\lambda$  profiles for ER network of size  $N = 10^3$ ,  $\langle d^{[2]} \rangle = 4$  when  $B_{ijk}$  is static (a-b) and adaptive (c-d) with  $\varepsilon = 1$  and  $\mu = 1$ .

between interacting oscillators have revealed intriguing structures and phenomena, for instance, the existence of cluster states [23–26] or mesoscale structures [27, 28], explosive synchronization arising from anti-Hebbian adaptation in monolayer networks [29] and interlayer Hebbian adaptation in multiplex networks [30].

The collective dynamics of man-made and natural complex systems represented by conventional graphs, for long, have been modeled using pairwise networked Kuramoto oscillators [31, 32]. When subjected to distinct adaptation-based features, including the Hebbian learning mechanism, the pairwise networked Kuramoto oscillators have led to a phenomenon termed first-order or explosive synchronization. A first-order transition sports an abrupt jump to the coherence, and then an irreversible abrupt collapse to the incoherence as the coupling strength between the interacting oscillators varies [29, 33–45]. In this work, breaking away from the traditional approach of assuming adaptation in pairwise coupling, we consider an adaptive higher-order cou-

\* iajaydeep@gmail.com

† sarikajalan9@gmail.com

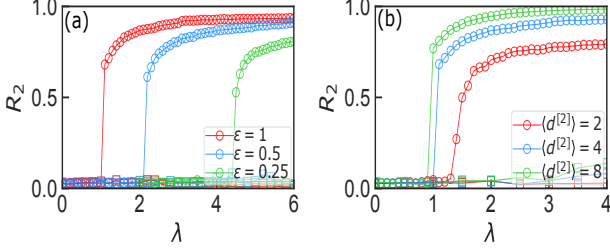


FIG. 2. (Color online) Impact of learning rate  $\varepsilon$  and mean 2-simplex degree  $\langle d^{[2]} \rangle$  on  $R_2 - \lambda$  transition in an ER network of size  $N = 10^3$ ,  $\mu = 1$  and  $\eta = 1$ .

pling among the interacting oscillators. In the proposed model, the dynamics of Kuramoto oscillators is driven by a triadic (three-way) coupling that adapts abiding by the Hebbian learning mechanism [30], i.e., a triadic coupling strengthens when the oscillators forming the triad are in phase and weakens when they are out of phase. Such dynamically adaptive triadic coupling gives rise to the first-order route to desynchronization, whose onset is entirely manageable through Hebbian learning parameters. A rigorous mean-field analysis presented successfully explains the dependence of the onset of abrupt desynchronization on Hebbian learning parameters.

## II. ADAPTIVE SIMPLICIAL COMPLEX

We consider a phase ensemble of Kuramoto oscillators subjected to adaptive higher-order interactions among them. The higher-order coupling interaction exercised among the oscillators is of triad (three-way) type encoded by 2-simplex (triangle) structure, whose weight dynamically adapt in accordance with a mechanism similar to Hebbian learning rule for pair-wise interaction [30]. The dynamical evolution of triplet weight assigned to a triad of nodes  $(i, j, k)$  having instantaneous phases  $\theta_{i,j,k}$  is governed by the following Hebbian-learning type adaptation

$$\dot{B}_{ijk} = \varepsilon \cos(\theta_j + \theta_k - 2\theta_i) - \mu B_{ijk}, \quad (1)$$

where constants  $\varepsilon \in [0, 1]$  and  $\mu > 0$  are learning enhancement rate and saturation rate, respectively. The cosine term implies that the coupling weight  $B_{ijk}$  tends to increase if triadic oscillators  $(i, j, k)$  are in phase, while it tends to decrease if they are out of phase. The linear saturating term  $\mu B_{ijk}$  refrains the coupling weight from increasing or decreasing without any bound. The phase evolution of Kuramoto oscillators under the impression of such triadic (triplet) interaction is ruled by

$$\dot{\theta}_i = \omega_i + \frac{\lambda}{2\langle d^{[2]} \rangle} \sum_{k=1}^N \sum_{j=1}^N B_{ijk} \sin(\theta_j + \theta_k - 2\theta_i), \quad (2)$$

where natural frequency  $\omega_i$  ( $i=1, \dots, N$ ) of each oscillator  $i$  is drawn randomly from a uniform or unimodal distribution  $g(\omega)$ , and  $\lambda$  is uniform coupling strength among

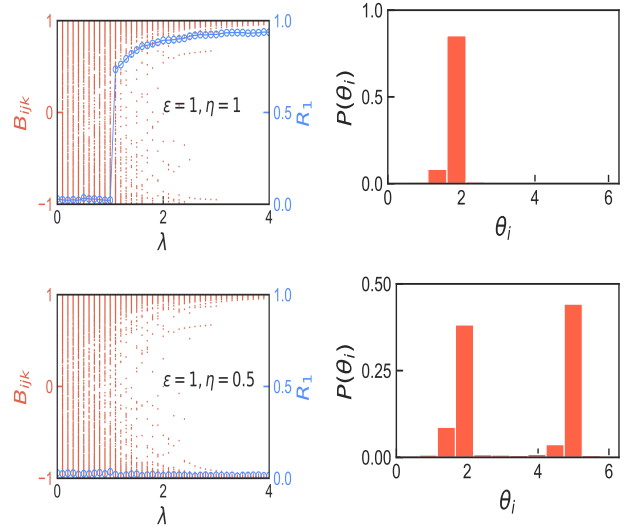


FIG. 3. (Color online) Stationary triplet weights  $B_{ijk}$  and stationary phases in an ER network for different values of  $\eta$ . The stationary phases corresponds to  $\lambda = 3$ . Other network parameters are  $N = 10^3$ ,  $\langle d^{[2]} \rangle = 4$ ,  $\varepsilon = 1$  and  $\mu = 1$ .

the interacting nodes. Here,  $B$  is an adjacency tensor of 2-simplex that encodes the topology of the network, i.e.,  $B_{ijk} = 1$  if there is a triadic (triplet) interaction among the nodes  $(i, j, k)$ , otherwise  $B_{ijk} = 0$ . The number of triangles in the network a node is part of, is defined as 2-simplex degree  $d_i^{[2]} = \frac{1}{2!} \sum_{j,k=1}^N B_{ijk}$ , and  $\langle d^{[2]} \rangle$  denotes the mean 2-simplex degree.

Eq. (1) and Eq. (2) together determine the collective dynamics of triadic networked oscillators. To capture the degree of synchronization among the triadic interacting oscillators in the network, we use the following generalized order parameter

$$Z_m = R_m e^{i\psi_m} = \frac{1}{N} \sum_{j=1}^N e^{im\theta_j}, \quad (3)$$

where choices of  $m=1$  and  $m=2$  yield one-cluster and two-clusters (or anti-phase clusters) order-parameters, respectively.

## III. NUMERICAL ASSESSMENT

In this section, we present the numerical outcomes observed for the two order parameters and also discuss the microscopic dynamics of the triplet weights. Here, we construct the 2-simplex structures by pinpointing each distinct triangle or triplet from the 1-simplex (Erdős-Rényi random graph) structures. We then simulate the phase and weight dynamics given by Eqs. (1) and (2) on the 2-simplex structures and compute the order parameters given by Eq. (3). The natural frequencies  $\omega_i$  of the nodes are drawn uniform randomly in the range  $[-0.5, 0.5]$ , if otherwise mentioned elsewhere. Fig. 1 illustrates the behavior of order parameters  $R_1$  and  $R_2$  against both adiabatic decrease and adiabatic increase

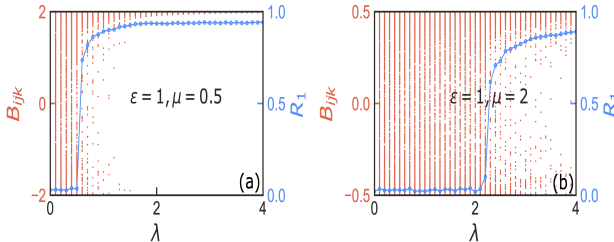


FIG. 4. (Color online) Stationary triplet weights  $B_{ijk}$  for an ER random network for different values of  $\mu$ . Other network parameters are  $N = 10^3$ ,  $\langle d^{[2]} \rangle = 4$ ,  $\varepsilon = 1$  and  $\eta = 1$ .

in  $\lambda$ . At a large  $\lambda$ , a uniformly selected fraction  $\eta$  of the nodes have their initial phases assigned to  $\theta_i(0) = 0$  and the rest,  $(1 - \eta)$ , assigned to  $\theta_i(0) = \pi$ . The initial weights  $B_{ijk}(0)$  are then determined by  $B_{ijk}(0) = (\varepsilon/\mu) \cos[\theta_j(0) + \theta_k(0) - 2\theta_i(0)]$ . At first,  $\lambda$  is adiabatically decreased until  $\lambda = 0$  is reached and then adiabatically increased to a large value.

*a. The role of Hebbian plasticity:* The behavior of  $R_1$  and  $R_2$  as a function of  $\lambda$  (see Fig. 1) illustrates how the onset of abrupt desynchronization is affected under the impression of adaptive evolution of triplet weights. The nature of abrupt desynchronization when the coupling weights  $B_{ijk}$  are static (i.e., in the absence of Eq. (1)), is shown in Figs. 1(a) & 1(b). The backward critical coupling strength  $\lambda_c$  at which the abrupt desynchronization takes place in both  $R_1$  and  $R_2$  increases with the increase in phase asymmetry ( $\eta = 0.5$  yields maximum asymmetry). Under the impression of triplet weight adaptation,  $R_1$  and  $R_2$  still adopt the abrupt desynchronization transition route, however the critical point  $\lambda_c$  is found to remain unaffected of the fraction  $\eta$  as shown in Figs. 1(c) & 1(d). The phase asymmetry  $\eta$  does affect the degree of synchronization for  $R_1$ . The maximum value to which  $R_1$  plateaus (at large  $\lambda$ ) decreases with the increase in the level of asymmetry, i.e.,  $\eta = 0.5$  (maximum asymmetry) yields  $R_1 \simeq 0$  while  $\eta = 1$  (no asymmetry) yields a larger  $R_1$ . Nevertheless, order-parameter  $R_2$  remains independent of initial phase asymmetry  $\eta$ . Moreover, both  $R_1$  and  $R_2$  do not see transition to a synchronous state with increment in  $\lambda$  and remain in the incoherent state for any  $\lambda > 0$ .

*b. Impact of learning rate and mean 2-simplex degree:* Additionally, we demonstrate the effect of learning rate  $\varepsilon$  and mean 2-simplex degree  $\langle d^{[2]} \rangle$  on the nature of synchronization in Fig. 2. As the learning rate  $\varepsilon$  is gradually decreased, the onset of first-order desynchronization transition takes place at higher values of critical coupling strength  $\lambda_c$  as shown in Fig. 2(a). Thus, the learning rate  $\varepsilon$  provides control over the onset of desynchronization. Moreover, the mean triplet connectivity  $\langle d^{[2]} \rangle$  also affect the jump height of the abrupt desynchronization (see Fig. 2(b)). As  $\langle d^{[2]} \rangle$  is increased, more and more triplets interactions are involved and lead to even greater amount of frustration among the nodes, which in turn increase the height of abrupt jump. A very low triplet connectivity  $\langle d^{[2]} \rangle = 2$  amounts to a negligible frustration among the nodes, hence it gives rise to a second-order

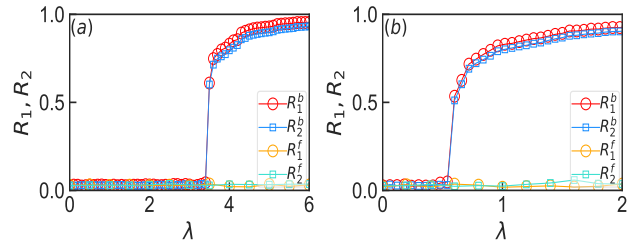


FIG. 5. (Color online)  $R_1 - \lambda$  and  $R_2 - \lambda$  profiles for ER network simulated with (a) Gaussian  $g(\omega)$  with half-width at half-maximum  $\Delta=1$  and (b) Lorentzian  $g(\omega)$  with  $\Delta=0.1$ . Other network parameters are  $N=10^3$ ,  $\langle d^{[2]} \rangle = 8$ ,  $\varepsilon = 1$ ,  $\mu = 1$  and  $\eta = 1$ .

transition.

*c. Stationary triplet weights and phases:* The microscopic dynamics of stationary weights and stationary phases during the backward sweep of  $\lambda$  are presented in Fig. 3 for different values of  $\eta$ . For  $\eta = 1$ , initial weights are  $B_{ijk}(0) = \varepsilon/\mu$  and as strength  $\lambda$  is gradually decreased, a gradually increasing number of  $B_{ijk}$  starts shifting away from  $\varepsilon/\mu$  towards  $B_{ijk} = 0$ . At the critical point  $\lambda_c$ , all  $B_{ijk}$  get uniformly scattered between  $-\varepsilon/\mu$  and  $\varepsilon/\mu$  and remain scattered so in the incoherent state until  $\lambda = 0$  is reached. The stationary phases corresponding to  $\lambda > \lambda_c$  remain locked to form a single peak distribution. However for  $\eta = 0.5$ , almost equal-half populations of  $B_{ijk}$  are initially set to  $-\varepsilon/\mu$  and  $\varepsilon/\mu$ . A gradual decrease in  $\lambda$  shifts a gradually increasing fraction of  $B_{ijk}$  towards 0. At the critical point, the entire  $B_{ijk}$  population now get scattered between  $-\varepsilon/\mu$  and  $\varepsilon/\mu$ . The stationary phases corresponding to  $\lambda > \lambda_c$  remain almost equally divided into two-clusters at a phase-difference of  $\pi$ .

*d. Impact of saturation rate  $\mu$ :* The impact of parameter  $\mu$  on stationary triplet weights is shown in Fig. 4. The ratio  $\varepsilon/\mu$  determines the lower and upper bounds for the stationary weights  $B_{ijk}$ , which can be corroborated from Eq. (1) in the steady state. Parameter  $0 < \mu \leq 1$  ( Fig. 4(a)) yields higher weight bounds which causes desynchronization at an early coupling strength. On the other hand,  $\mu > 1$  ( Fig. 4(b)) yields lower weight bounds which leads to the desynchronization at rather higher coupling strength. Therefore,  $\mu$  also serves as a control parameter in determining the onset of abrupt desynchronization.

*e. Effect of different frequency distributions:* The occurrence of first-order desynchronization while considering Gaussian  $g(\omega) = \frac{1}{\Delta\sqrt{2\pi}} \exp(-\omega^2/2\Delta^2)$ ; with half-width at half-maximum  $\Delta=1$  and Lorentzian  $g(\omega) = \frac{\Delta}{\pi(\omega^2 + \Delta^2)}$  with  $\Delta=0.1$  are shown in Fig. 5. The values of backward critical coupling strength for these distributions are different than those observed for uniform  $g(\omega)$ .

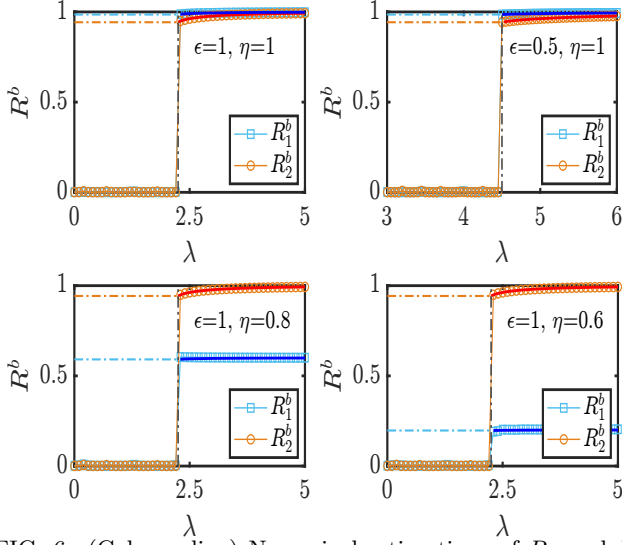


FIG. 6. (Color online) Numerical estimations of  $R_1$  and  $R_2$  against  $\lambda$  for an all-to-all connected network and their analytical predictions in solid blue ( $R_1$ ) and solid red ( $R_2$ ) lines, respectively, given by Eq.(11) for different values of learning rate  $\epsilon$  and initial phase asymmetry  $\eta$  while  $\mu = 1$ .

#### IV. ANALYTICAL DISCUSSION:

To gain the theoretical insight of the underlying dynamics of adaptive 2-simplex complexes, we turn our focus to the evolution of all-to-all connected network modeled as

$$\dot{\theta}_i = \omega_i + \frac{\lambda}{N^2} \sum_{k=1}^N \sum_{j=1}^N B_{ijk} \sin(\theta_j + \theta_k - 2\theta_i). \quad (4)$$

The system can achieve its stationary state only when both triplet weights and phases achieve their respective stationary states. The stationary triplet weights,  $\dot{B}_{ijk} = 0$  in Eq.(1), are given by

$$B_{ijk} = \frac{\varepsilon}{\mu} \cos(\theta_j + \theta_k - 2\theta_i) = \frac{\varepsilon}{\mu} \cos(\Delta\theta_{ijk}). \quad (5)$$

Eq. 5 suggests that  $B_{ijk}$  settles on two weight populations in the steady state, one  $B_{ijk} = \varepsilon/\mu$  corresponding to  $\Delta\theta_{ijk} = 0$  and  $B_{ijk} = -\varepsilon/\mu$  corresponding to  $\Delta\theta_{ijk} = \pi$ . For that matter, an asymmetric initial phase population comprising 0 or  $\pi$  phases with a probability  $\eta$  and  $1-\eta$ , respectively, is taken into account. The Eq. (4) can be re-expressed in terms of mean-field parameters using Eqs. (3) and (5) as

$$\dot{\theta}_i = \omega_i + bq \sin(2\psi_2 - 4\theta_i); \quad b = \frac{\varepsilon}{2\mu} \quad \& \quad q = \lambda R_2^2. \quad (6)$$

Since phases in a frame rotating with the average intrinsic frequency  $\dot{\Psi}_m$  are given by  $\theta_i = \theta_i + \dot{\Psi}_m t$ . Nevertheless, considering a non-rotating frame with  $\dot{\Psi}_m = 0$  and setting the average phase  $\Psi_m = 0$  by selecting appropriate initial phases, the equilibrium points in synchronous

state  $\dot{\theta}_i = 0$  ( $|\omega_i| \leq bq$ ) are determined by

$$\sin(4\theta_i^*) = \frac{\omega_i}{bq}; \quad \cos(2\theta^*) = \pm \sqrt{\frac{1}{2} \left[ 1 + \sqrt{1 - \frac{\omega^2}{b^2 q^2}} \right]}, \quad (7)$$

where  $\eta$  and  $(1 - \eta)$  denote a constant probability ( $\eta(\omega_i) = \eta$ ) with which the initial phases are set to 0 and  $\pi$ , respectively. Hence, the order parameter (Eq. (3)) for the locked oscillators in continuum limit can be expressed as

$$R_m = \int_{|\omega| \leq bq} d\omega g(\omega) \int_0^{2\pi} d\theta e^{im\theta} [\eta \delta(\theta - \theta^*) + (1 - \eta) \delta(\theta - \theta^* - \pi)]. \quad (8)$$

Further mathematical simplifications yield the real part of the order parameters as

$$R_1 = \int_{|\omega| \leq bq} d\omega g(\omega) (2\eta - 1) \cos(\theta^*),$$

$$R_2 = \int_{|\omega| \leq bq} d\omega g(\omega) \cos(2\theta^*). \quad (9)$$

Substitution of  $\cos(\theta^*)$  and  $\cos(2\theta^*)$  from Eq. (7) into Eq. (9) yields

$$R_1 = (2\eta - 1) \int_{|\omega| \leq bq} d\omega g(\omega) \cos \left[ \frac{1}{4} \arcsin \left( \frac{\omega}{bq} \right) \right],$$

$$R_2 = \int_{|\omega| \leq bq} d\omega g(\omega) \sqrt{\frac{1}{2} \left[ 1 + \sqrt{1 - \frac{\omega^2}{b^2 q^2}} \right]}. \quad (10)$$

Considering a uniform distribution  $g(\omega) = \frac{1}{2\Delta}$ , following expressions for the two order parameters are obtained

$$R_2 = \frac{\sqrt{2}b^2 q^2}{3\Delta^2} \left( 1 - \sqrt{1 - \frac{\Delta^2}{b^2 q^2}} \right) \left( 2 + \sqrt{1 - \frac{\Delta^2}{b^2 q^2}} \right) \sqrt{1 + \sqrt{1 - \frac{\Delta^2}{b^2 q^2}}},$$

$$R_1 = 2(2\eta - 1) \frac{bq}{\Delta} \left[ \frac{1}{3} \sin \left( \frac{3}{4} \arcsin \left( \frac{\Delta}{bq} \right) \right) + \frac{1}{5} \sin \left( \frac{5}{4} \arcsin \left( \frac{\Delta}{bq} \right) \right) \right]. \quad (11)$$

It is apparent from Eq. (11) that only order parameter  $R_1$  is impacted by the change in the initial phase asymmetry  $\eta$  while  $R_2$  remains independent of it. The backward end points of  $R_1 - \lambda$  and  $R_2 - \lambda$  traces are obtained by setting

$\Delta = bq = b\lambda_c R_{2c}^2$ :

$$R_{1c} = 0.98(2\eta - 1), \quad R_{2c} = \frac{2\sqrt{2}}{3}, \quad \lambda_c = \frac{9\mu\Delta}{4\epsilon}. \quad (12)$$

It is apparent that the critical coupling strength  $\lambda_c$  for the onset of desynchronization is the function of Hebbian plasticity rates  $\epsilon$  and  $\mu$ . The analytical predictions (Eq. (11)) for  $R_1$  and  $R_2$  are plotted in Fig. 6 for different values of  $\epsilon$  and  $\eta$ . They are fairly in good agreement with their respective numerical estimations. The values of critical points  $\lambda_c$  and  $R_{1c}$  and  $R_{2c}$  are also shown matching their respective numerical assessments.

## V. CONCLUSION

We have studied the impact of weight adaptation in higher-order triadic interaction on synchronization transition in an ensemble of Kuramoto oscillators. The adaptation exercised in triadic coupling is inspired by the Hebbian learning mechanism, i.e., a triplet weight tends to increase when the nodes forming the triplet are in phase and decrease when they are out of phase. The dynamical evolution of such Hebbian learning ruled triadic couplings leads to a first-order desynchronization in the network. The triggering point of the emerging abrupt desynchronization is manageable through Hebbian learning parameters, i.e., the learning rate and saturation rate. The ini-

tial phase asymmetry regulates the one-cluster order parameter while the two-clusters order parameter remains independent of it. Also, the triplet weights remain uniformly distributed in the incoherent state, whereas they form one-cluster or two-clusters depending on the initial phase asymmetry. The rigorous mean-field analysis successfully explains the behavior of one-cluster and two-clusters order parameters under the imprint of the Hebbian learning type adaptation of 2-simplex complexes.

All the investigations featuring adaptation so far have revolved around considering a pair-wise interaction between the interacting oscillators. The present study would be advantageous in understanding the role of adaptive higher-order coupling in underlying dynamics in the brain and social interaction networks. The proposed model also opens an avenue for investigating the imprint of concurrent adaptation in dyadic and triadic couplings on the synchronization dynamics of the phase oscillators.

## ACKNOWLEDGMENTS

S.J. thanks Government of India, Council of Scientific & Industrial Research (CSIR) Grant No. 25(0293)/18/EMR-II and Board of Research in Nuclear Sciences (BRNS) Grant No. 37(3)/14/11/2018-BRNS/37131 for financial support. A.D.K. acknowledges the Government of India, Council of Scientific & Industrial Research (CSIR) Grant No. 25(0293)/18/EMR-II for the RA fellowship.

---

[1] G. Petri, P. Expert, F. Turkheimer, R. Carhart-Harris, D. Nutt, P. J. Hellyer and F. Vaccarino, *J. R. Soc. Interface* **11**, 20140873 (2014)

[2] A. R. Benson et al., *Proc. Natl. Acad. Sci. U.S.A.* **115**, E11221 (2018)

[3] I. Iacopini, G. Petri, A. Barrat, and V. Latora *Nat. Commun.* **10**, 2485 (2019)

[4] J. T. Matamalas, S. Gómez and A. Arenas *Phys. Rev. Research* **2**, 012049(R) (2020)

[5] V. Salnikov, D. Cassese, and R. Lambiotte *Eur. J. Phys.* **40**, 014001 (2018)

[6] J.H.C. Whitehead *Proc. London Math. Soc.* **45** 243–327 (1939)

[7] T. Tanaka and T. Aoyagi, *Physical Review Letter* **106**, 224101 (2011)

[8] P. S. Skardal and A. Arenas, *Phys. Rev. Lett.* **122**, 248301 (2019)

[9] C. Xu, X. Wang and P. S. Skardal, *Physical Review Research* **2**, 023281 (2020)

[10] A. P. Millán, J. J. Torres and G. Bianconi *Phys. Rev. Lett.* **124**, 218301 (2020)

[11] P. S. Skardal and A. Arenas *Communication Physics* **3**, 218 (2020)

[12] M. Lucas, G. Cencetti and F. Battiston *Physical Review Research* **2**, 033410 (2020)

[13] F. Battiston, G. Cencetti, I. Iacopini, V. Latora, M. Lucas, A. Patania, Jean-Gabriel Young and G. Petri, *Physics Reports* **874**, 1–92 (2020)

[14] R. Ghorbanchian, J. G. Restrepo, J. J. Torres and G. Bianconi, *Communication Physics* **4**, 120 (2021)

[15] C. Xu and P. S. Skardal, *Physical Review Research* **3**, 013013 (2021)

[16] M. Chutani, B. Tadić, and N. Gupte, *Physical Review E* **104**, 034206 (2021)

[17] H. Sun and G. Bianconi *Physical Review E* **104**, 034306 (2021)

[18] E. Shimizu, Y. P. Tang, C. Rampon and J. Z. Tsien, *Science* **290**, 1170–1174 (2000)

[19] L. F. Abbott and S. B. Nelson, *Nature Neuroscience* **3** (11) 1178–1183 (2000)

[20] D. O. Hebb, *The Organization of Behavior* (New York: John Wiley & Sons) (1949)

[21] H. Markram, J. Lübke, M. Frotscher and B. Sakmann, *Science* **275** 213–215 (1997)

[22] L. I. Zhang, H. W. Tao, C. E. Holt, W. A. Harris and M. Poo, *Nature* **395** 37–44 (1998)

[23] R. K. Niyogi and L. Q. English, *Phys. Rev. E* **80**(6), 066213 (2009)

[24] T. Aoki and T. Aoyagi, *Physical Review Letter* **102**, 034101 (2009)

[25] R. Berner, J. Sawicki and E. Schöll, *Phys. Rev. Lett.* **124**(8) 088301 (2020)

- [26] R. Berner, S. Vock, E. Schöll and S. Yanchuk, *Phys. Rev. Lett.* **126**(2), 028301 (2021)
- [27] R. Gutiérrez, A. Amann, S. Assenza, J. Gómez-Gardeñes, V. Latora and S. Boccaletti, *Phys. Rev. Lett.* **107** 234103 (2011)
- [28] E. Pitsik, V. Makarov, D. Kirsanov, N. Frolov, M. Goremyko, X. Li, Z. Wang, A. Hramov and S. Boccaletti, *New Journal of Physics* **20**, 075004 (2018)
- [29] V. Avalos-Gaytán, J. A. Almendral, I. Leyva, F. Battiston, V. Nicosia, V. Latora and S. Boccaletti, *Phys. Rev. E* **97**(4) 042301 (2018)
- [30] A. D. Kachhvah, X. Dai, S. Boccaletti and S Jalan, *New Journal of Physics* **22** 122001 (2020)
- [31] Y. Kuramoto, *International Symposium on Mathematical Problems in Theoretical Physics, Lecture Notes in Physics* **39** (1975)
- [32] J. A. Acebrón, L. L. Bonilla, C. J. Pérez Vicente, F. Ritort and R. Spigler *Rev. Mod. Phys.* **77**(1) 137–185 (2005)
- [33] H. A. Tanaka, A. J. Lichtenberg and S. Oishi, *Phys. Rev. Lett.* **78**(11) 2104–2107 (1997)
- [34] J. R. Pomerening, E. D. Sontag and Jr J. E. Ferrell, *Nature Cell Biology* **5** 346–351 (2003)
- [35] J. Gómez-Gardeñes, S. Gómez, A. Arenas and Y. Moreno, *Physical Review Letter* **106**(12) 128701 (2011)
- [36] I. Leyva, R. Sevilla-Escoboza, J. M. Buldú, N. I. Sendiña, J. Gómez-Gardeñes, A. Arenas, Y. Moreno, S. Gómez, R. Jaimes-Reátegui and S. Boccaletti, *Physical Review Letter* **108**(16) 168702 (2012)
- [37] M. M. Danziger, O. I. Moskalenko, S. A. Kurkin, X. Zhang, S. Havlin and S. Boccaletti, *Chaos* **26** 065307 (2016)
- [38] V. K. Chandrasekar, M. Manoranjani and S. Gupta, *Phys. Rev. E* **102**(1) 012206 (2020)
- [39] C. Kuehn and C. Bick, *Science Advances* **7**(16) eabe3824 (2021)
- [40] M. M. Danziger, I. Bonamassa, S. Boccaletti and S. Havlin, *Nature Physics* **15**(2) 178–185 (2019)
- [41] I. Shepelev, A. Bukh, G. Strelkova and V. Anishchenko, *Chaos, Solitons & Fractals* **143** 110545 (2021)
- [42] A. Kumar and S. Jalan *Chaos* **31**, 041103 (2021)
- [43] P. Khanra and P. Pal, *Chaos, Solitons & Fractals* **143** 110621 (2021)
- [44] N. Frolov and A. Hramov, *Chaos* **31**, 063103 (2021)
- [45] N. Frolov and A. Hramov, *Chaos Solitons & Fractals* **147**, 110955 (2021)